HEAVY-ION CYCLOTRON GYMNASTICS AND ASSOCIATED BEAM DYNAMICS ISSUES

N. Fukunishi, Nishina Center for Accelerator-Based Science, RIKEN, Wako, Japan

Abstract

After a brief introduction to heavy-ion cyclotrons, their beam dynamics are outlined, with an emphasis on the space-charge effect, and important achievements in both proton and heavy-ion cyclotrons are described.

INTRODUCTION

The first heavy-ion acceleration using a cyclotron was a 50-MeV ^{12}C beam accelerated by the 37-inch Berkeley cyclotron in 1940 [1]. The beam intensity was only 8 particles/s. To illustrate the subsequent development of heavy-ion cyclotrons, data compiled by Livingston [1] (up to 1969) and data taken from the "List of Cyclotrons" published in 2004 [2] are combined in Fig. 1. Each cyclotron is classified according to its type and first-beam date (or the date of acceleration of the heavy-ion beam as listed in Livingston's tables). Although Fig. 1 is an incomplete historical review, we can observe a remarkable increase in energy. Beam intensity seems to stay relatively constant, but that is because the beam intensity of very light ions was high even in the very early stages of cyclotron history. However, beam intensities for heavier ions, such as ^{48}Ca and ^{238}U, have greatly increased thanks to advances in ion sources. Because recent low-energy nuclear physics experiments pursue very rare events, beam intensity has become a crucial issue.

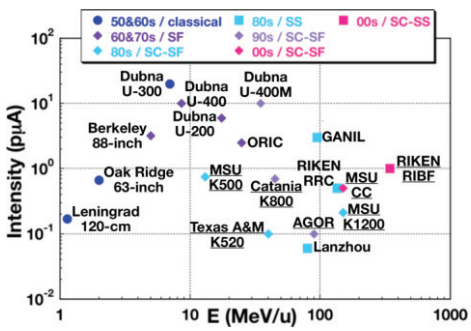

Figure 1: Historical development of heavy-ion cyclotrons.

Nuclear physics is one of the most important applications of heavy-ion cyclotrons: unstable nuclei far from the β-stability line are being extensively studied and many new superheavy elements have been synthesized at JINR FLNR [3]. Heavy-ion beams are also widely used for material modification and analysis (PIXE, RBS, etc.) [4]. The high biological effectiveness of energetic heavy ions has also enabled applications in medical science, biology, agriculture and so on. A compact superconducting cyclotron capable of delivering a 400 MeV/amu carbon beam for cancer therapy has been designed by an IBA-JINR collaboration [5]. Also, wide variety of plant mutations have been induced by energetic light ions [6] accelerated in the RIKEN Ring Cyclotron (RRC) [7]. The reviews of Onishchenko [8] and Goto [9] provide more detail.

BASIC FEATURES OF CYCLOTRONS

Types of Cyclotron

The classical cyclotron invented by Lawrence [10] employed an azimuthally uniform and radially decreasing magnetic field to produce approximate isochronism and vertical stability of particle motion. However, as Bethe pointed out [11], the relativistic mass increase of ions requires a radially increasing field, which impairs vertical stability. The inventions of synchrocyclotrons [12-14] and Thomas cyclotrons solved this conflict. Thomas proposed the use of an azimuthally varying field [15] (AVF) for an isochronous magnetic field. In this case, an ion's orbit is non-circular and ions can experience edge focusing in the vertical direction. The Thomas cyclotron, also called the isochronous or sector focusing cyclotron, was first demonstrated by Richardson but this fact was classified until 1956 [16]. A further modification of the isochronous magnetic field by using spirally ridged magnet poles was proposed by Kerst et al. [17], which is effective to increase vertical focusing. Cyclotrons with spirally ridged poles are widely used, especially for high-energy cyclotrons.

To realize meson factories, a separate sector or ring cyclotron was proposed [18,19]. A single magnet producing an isochronous magnetic field is divided into sector magnets which are arranged in a ring with spaces between them. This configuration loses one virtue of cyclotrons, compactness, but gains stronger vertical focusing and higher acceleration voltages because azimuthal modulation of the isochronous magnetic field is much stronger than in AVF cyclotrons and high-voltage resonators can be installed in the spaces between the sector magnets. Thus, separate sector cyclotrons are used to produce high-intensity beams. A separated orbit cyclotron (SOC), proposed by Russell [20] and Martin [21], and demonstrated by Trinks [22], is another important variation, but there are no SOCs routinely serving heavy-ion beams to users. For more details of cyclotron development, many review articles are available: for example, the review by Craddock [16].

Among the currently working heavy-ion cyclotrons, GANIL, IMP-Lanzhou, RCNP and RIBF use separate sector cyclotrons, U-400 and U-400m of JINR FLNR are normal conducting AVF cyclotrons, and K500 and K1200 (MSU/NSCL), K500 (TAM), K800 (Catania) and AGOR (K600) are very compact superconducting AVF-type cyclotrons. A coupled cyclotron system at MSU/NSCL accelerates heavy ions up to 160 MeV/amu, though their

ISBN 978-3-95450-173-1

cyclotrons use magnets weighing 90 ~ 240 tons, which are one order of magnitude smaller than those used in normal-conducting separate sector cyclotrons.

Beam Optics in Cyclotrons

In a cyclotron, beam optics is determined by a given isochronous magnetic field and depends on ion energy. If we neglect acceleration, a periodic solution, representing an equilibrium orbit of an ion moving under the isochronous magnetic field is obtained. Betatron tunes and beta functions can also be determined. Figure 2 shows tune diagrams for the four ring cyclotrons of RIBF for accelerating uranium ions up to 345 MeV/amu. Numerical methods are usually used to evaluate tunes, but the analytic expressions [23,24]

$$\nu_r^2 = 1 + n + O(N^{-2})\ \nu_z^2 = -n + \frac{1}{2}f^2(1 + 2\tan^2\theta) + O(N^{-2})$$

are widely used as a starting point in cyclotron design. Here, n, θ, f^2 and N are the field index, spiral angle, flutter and harmonic number of each Fourier component of the magnetic field. The flutter indicates strength of azimuthal modulation of the isochronous magnetic field. For an azimuthally uniform or azimuthally averaged isochronous magnetic field, the relation $B = B_0\gamma$ with constant B_0 holds and we obtain $n = \beta^2\gamma^2$ and $\nu_r = \gamma$. The vertical tune ν_z decreases as beam energy increases and vertical focusing is given by the $f^2(1 + 2\tan^2\theta)$ term.

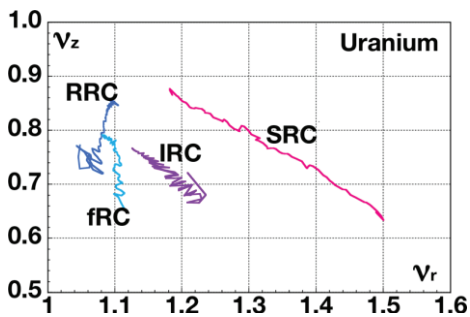

Figure 2: Tune diagrams of a 345 MeV/amu uranium beam in RIBF. A cascade of these four ring cyclotrons is used in practice.

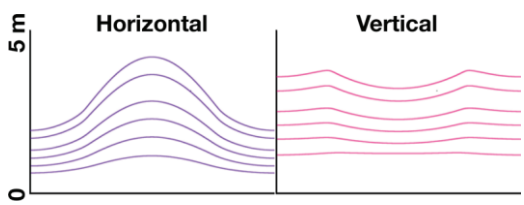

Figure 3: Beta functions of uranium ions accelerated by RRC from 0.7 to 10.8 MeV/amu. Beta functions of one unit cell starting from the valley center are shown for six different energies (from the bottom to top, 0.7, 1.3, 2.3, 3.4, 5.7 and 7.5 MeV/amu).

Beta functions ($\hat{\beta}$) increase in proportion to the ion's orbital radius and are modulated, to a certain extent, reflecting changes of focusing strength (see Fig. 3). The matched beam radius σ ($\sigma^2 = \hat{\beta}\varepsilon$) scales as $\sigma \propto \sigma_0/\gamma$ (σ_0 constant) if we use the smooth approximation $\hat{\beta} = R/\nu$. In any case, beam radiuses change gradually in both horizontal and vertical directions during acceleration, if a beam is matched to its eigen-ellipses at injection. Whether all the relevant matching conditions, such as emittance and dispersion matching, are fulfilled is examined by measuring the charge density distribution (turn pattern) of a beam.

INTENSITY LIMITING FACTORS OF HEAVY-ION CYCLOTRONS

Compared with the success of PSI that routinely accelerates a 1.3 MW proton beam [25,26], beam powers obtained by heavy-ion cyclotrons are limited to less than 10 kW [27-29]. Stetson et al. [29] classified the intensity-limiting factors of the MSU/NSCL coupled cyclotron system into three categories: source, stripper and power limited. The last of these can be generalized to include all the limits imposed by unacceptable beam loss in cyclotrons. At MSU/NSCL, medium-heavy metal elements such as Ni, Zr and Sn are source limited. At RIBF, 345A-MeV ^{48}Ca (415 pnA) and ^{70}Zn (123 pnA) beams are also source limited. Because the ion sources used there are not state-of-the-art, the present situation will be improved in the near future.

On the other hand, the remaining two factors will remain serious problems. Beam intensity for very heavy ions like uranium is frequently limited by stripper lifetime. The lifetime of carbon foils reported by Stetson [29] is less than a few minutes for a 7.7-MeV/amu ^{238}U beam with an intensity of 20 pnA. Our experience is typically less than 12 h for a 15-pnA ^{238}U beam at 10.8 MeV/amu. (The reason for this large discrepancy between the lifetimes of the two facilities is not understood.) To solve this lifetime problem, a helium gas stripper was successfully introduced [30] at RIBF. However, RIBF adopts a two-step charge-stripping scheme to accelerate uranium ions up to 345 MeV/amu. Rotating beryllium disks (~18 mg/cm^2) now serve as the second-stage charge-state stripper [31] at 50 MeV/amu and the beam-intensity limit is less than 150 pnA for a 50-MeV/amu uranium beam based on our operating experience. Beyond this, beryllium disks are not only seriously deformed but also crack due to heat deposited from the beam.

Although beam loss at injection and during acceleration sometimes causes serious problems [32], beam loss at extraction has been the major concern in cyclotron development. With the exceptions of charge-stripping extraction used at JINR FLNR [33], TRIUMF [34] and so on, an electrostatic deflector is widely used as the first stage of beam extraction. Because heavy-ion cyclotrons pursue versatility of ion species and beam energy, the use of deflectors is a reasonable choice at present. A septum electrode of the deflector is placed between the final turn to be extracted and the other turns. If separations between these turns are insufficient at extraction, sizable beam loss

ISBN 978-3-95450-173-1

occurs. The maximally allowed heat deposit on a septum electrode is typically about 0.3-0.5 kW, which eventually limits available beam intensity in high-power cyclotrons.

The beam-intensity limit imposed by a requirement for hands-on maintenance is usually higher than the present power limit for heavy-ion cyclotrons because energetic heavy ions produce much less radioactivity than energetic protons do [35].

MEASURES USED FOR CLEAN BEAM EXTRACTION

As mentioned above, insufficient turn separation at beam extraction causes sizable beam losses. The azimuthally averaged turn separation (ΔR) in cyclotrons is given by

$$\Delta R = \frac{qeV_{acc}}{mc^2}\frac{\gamma}{(\gamma^2-1)\nu_r^2}R$$

Here, m and qe are the mass and charge of the ion, respectively, V_{acc} is the acceleration voltage per turn, R is the average orbital radius and ν_r is the horizontal tune. So, a combination of a high acceleration voltage and a smaller average magnetic field is essential to obtain a sufficient turn separation—an approach that is adopted in PSI injector 2 [36]. However, heavy-ion cyclotrons have pursued high magnetic fields to realize higher-energy beams and their turn separations are not large enough for high-intensity beams. This is one of the difficulties in heavy-ion cyclotron design.

To overcome this difficulty, several measures are used [37,38], one of which is inducing coherent radial motions. Techniques that can be applied are precessional (off-centring) acceleration, regenerative acceleration, beam orbit expansion [39] and so on. RIBF routinely uses precessional acceleration, in which a coherent radial betatron motion is induced at injection. The turn pattern has alternating sparse- and dense-turn regions and the beam is extracted from a sparse-turn region by adjusting acceleration voltage.

The situation becomes more serious for small cyclotrons used as first-stage accelerators. In this case, the beam injected into the cyclotron is not well bunched. If we use an acceleration voltage in the form of a single sinusoidal wave, a long bunch experiences a banana-shaped deformation in the radial-longitudinal plane due to an energy spread caused by a time-varying acceleration voltage and dispersion of the applied isochronous magnetic field. This banana-shaped deformation reduces turn separation. Flat-topping resonators improve the uniformity of the acceleration voltage by producing decelerating RF fields working at a frequency which is an integer multiple of the acceleration voltage. Using a radially increasing accelerating field is also effective for long bunches. The radial increase of the electric field produces a time-dependent magnetic field in a polar direction. Leading (trailing) particles are deflected outward (inward) and are moved backward (forward) by the RF magnetic field. As a result, beam bunches are compressed in the longitudinal direction [40] and the energy spread is reduced.

However, the effectiveness of these measures is established for only low-intensity beams. Space-charge effects, in many cases, destroy the gain expected by these measures.

BEAM DYNAMICS IN CYCLOTRONS

Space-charge effects have been studied extensively for both proton and heavy-ion cyclotrons. A brief summary is given here.

Vortex Motion

Gordon [41] emphasized the importance of vortex motion induced by a strong radial-longitudinal coupling in cyclotrons. Assuming a uniform magnetic field and $\gamma\sim1$, particle motion relative to the bunch center is expressed in the rotating frame as

$$\frac{d\vec{v}}{dt}+\vec{\omega}\times\vec{v}=\frac{q}{m}\vec{E}.$$

Here, $\vec{E}$ and ω are the space-charge electric field and cyclotron angular frequency, respectively. Gordon discussed a steady state of the equation by neglecting the first term of the left side. (This corresponds to averaging out fast particle motions such as betatron oscillations.) In this case, we can easily understand a characteristic feature of the steady state under the space-charge force; in other words, particles move along an equipotential surface of the space-charge field. Gordon described two kinds of vortex motions: an overall vortex motion and a local vortex motion. The former occurs when neighboring turns overlap each other and equipotential surfaces extend in the radial direction over many adjacent bunches. The latter occurs when turns are separated. In this case, the orbital radius of a particle accelerated (decelerated) by the space-charge force increases (decreases) due to the isochronous magnetic field. An outer (inner) particle experiences an outward (inward) kick from the space-charge force and moves backward (forward). Hence, particles rotate around the bunch center. The local vortex motion washes out the energy gain obtained from the space-charge force.

The local vortex motion described by Gordon was later discovered as a “round beam”. Its existence was confirmed by a series of studies [42-44] for PSI injector 2. The reason why this discovery attracts much attention is that a round beam seems to keep its shape all the way to beam extraction and indicates the possibility of accelerating a beam bunch that is near its space-charge limit [45].

Kleeven’s theoretical work [46] is based on a smooth approximation to the isochronous magnetic field and Sacherer’s linearization technique [47] applied to space-charge forces. Kleeven derived a set of equations describing the time evolution of all the second moments relevant to particle motion and demonstrated the existence of a stationary solution with rotational symmetry, that is, a round beam.

ISBN 978-3-95450-173-1

Bertrand and Ricaud [48] also employed a linear analysis as their starting point. For a non-relativistic particle (mass m and charge q) moving under a uniform magnetic field (B_z), with the assumption that a beam bunch is a uniformly charged sphere, the equation of motion in a radial-longitudinal plane is given by

$$\ddot{z} = i\omega\dot{z} + \lambda(z - z_0).$$

Here a complex variable $z = x + iy$ has been introduced, where x and y denote radial and longitudinal coordinates in the laboratory frame, respectively. The subscript 0 indicates the bunch center, ω is the cyclotron angular frequency, λ is defined as $\lambda = qk/m$, and k is the gradient of the space-charge electric field. The gradient is given by $k = Q/4\pi\epsilon_0 r_0^3$, where Q and r_0 are the charge and radius of the assumed charged sphere. The solution is easily obtained as

$$z - z_0 = Ae^{i\omega\nu_+ t} + Be^{i\omega\nu_- t}.$$

Here, tunes $\nu_\pm$ are determined by solving the characteristic equation $\omega^2\nu_\pm^2 - \omega^2\nu_\pm + \lambda = 0$ to obtain

$$\nu_\pm = \frac{1 \pm \sqrt{1 - 4\lambda\omega^{-2}}}{2}.$$

In this model, particle motion is described by a superposition of sinusoidal waves. Examples of particle motion are shown in Fig. 4. Using these solutions, Bertrand and Ricaud constructed a transfer matrix and obtained a stationary solution of the beam matrix. Hence the K-V distribution [49] was determined in this simplified model. The stationary solution should fulfil several matching conditions on the parameters describing a four-dimensional phase-space ellipse. One of them is that the distribution should be rotationally symmetric in the radial-longitudinal plane; hence, the assumption of a uniformly charged sphere is consistent with the stationary condition. Starting with these matching conditions, Bertrand and Ricaud investigated the stability of a round beam that has a finite six-dimensional emittance (inside a ellipse) in their fully three-dimensional space-charge simulations. They reported that a stable round beam, not exhibiting pulsation and halo formation, was obtained after an adjustment.

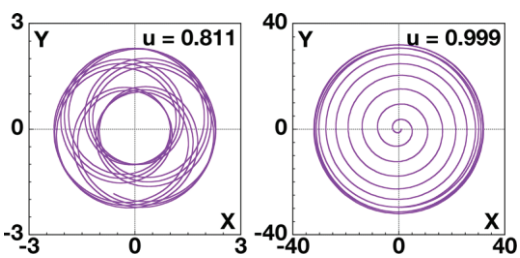

Figure 4: Solutions of the linearized equation of Bertrand and Ricaud. The parameter u is an index of the space-charge effect, defined by $u = 4\lambda\omega^{-2}$.

In the linear analysis, particle motion is bound for only $4\lambda/\omega^2 < 1$ and a particle's orbital radius increases exponentially beyond the space-charge limit. This is, of course, unrealistic. For particles outside the beam core, an analysis of Chasman and Baltz [50] can be applied. In their model, the electric field experienced by a test particle moving outside the beam core is $E(\rho) = Q\vec{\rho}/4\pi\epsilon_0\rho^3$, where Q is the charge of the beam core and ρ is the radial distance of the test particle from the center of the beam core. Chasman and Baltz obtained an exact analytic solution using elliptic integrals and also presented an intuitively understandable approximate solution. In this case, a test particle placed at the surface of the beam core with no kinetic energy undergoes a cloverleaf-shaped motion and all particles are bound by a strong magnetic field.

SPACE-CHARGE SIMULATION

To analyze particle motion in realistic cyclotrons, numerical simulations are necessary; only then can effects from acceleration, the strongly modulated magnetic fields of separate sector cyclotrons, neighboring turns and so on be precisely taken into account. Many simulation codes have been developed [43,48,51-54] and one of the most advanced is OPAL [55]. We have also developed a classical particle-in-cell code in order to reproduce important results made by previous authors. Characteristic features of our code include Runge-Kutta integration for the time evolution of particle motion, evaluation of the space-charge force in the particle-rest frame (only the electrostatic potential is included), use of an area-weighted charge density distribution for Poisson's equation, a DFT-based direct Poisson solver. The Poisson computation box is chosen to be a rectangular parallelepiped and the potential is set to zero at two vertical boundaries simulating a beam chamber. The longitudinal boundary condition is virtually open and the radial boundary condition is chosen carefully. The number of test particles used is 10^5 to 10^6.

We made space-charge simulations for uranium ions accelerated by RRC with an assumption of separated turns. While a long bunch exhibits a spiral galaxy-shaped distribution even for beam intensities much less than the space-charge limit (Fig. 5(a)), a short bunch remains round (Fig. 5(b)). This result reproduces preceding work [43] and demonstrates the effectiveness of the round-beam acceleration scheme [45].

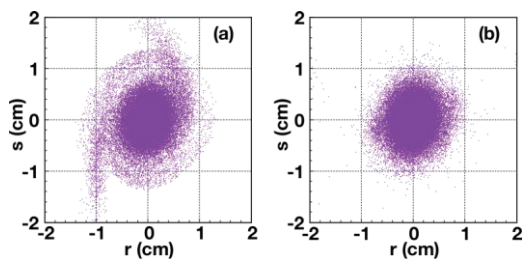

Figure 5: Particle distributions in horizontal (r) and longitudinal (s) planes for $^{238}U^{35+}$ 10.8 MeV/amu beams with intensities and initial phase widths of (a) 1 pμA and 6°and (b) 5 pμA and 3°.

The effectiveness of accelerating much longer bunches ($\Delta\phi$ = ~20°) using flat-topping resonators should be

ISBN 978-3-95450-173-1

investigated because the charge density of bunches substantially decreases and the linear part of the space-charge force can be compensated by shifting the phases of the flat-topping resonators. Our simulations for RRC show that a long-bunch acceleration scheme gives a lower intensity limit, as in the case of PSI injector 2. However, this does not mean the round-beam scheme is always superior to the long-bunch scheme. A formula recently proposed for separated turns by Baartman [56] predicts an intensity limit of 2.6 pμA for a 345-MeV/amu uranium beam accelerated in SRC [57], our final stage accelerator. On the other hand, a space-charge simulation predicts an intensity limit of 6 pμA [58] for a uranium beam consisting of long bunches using a flat-topping resonator. Of course these two estimations do not strictly employ the same criteria for allowable beam loss and also include some uncertainties, but the reason why the latter simulation yields a similar intensity limit is that the bunch is very long (~16 cm at extraction).

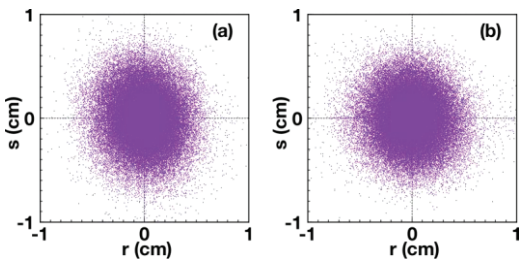

Figure 6: Particle distributions at extraction for a 10.8-MeV/amu $^{238}U^{35+}$ beam in case of the 24.33 MHz acceleration scheme. Results of (a) a 5-bunch simulation and (b) a 7-bunch simulation are shown.

A round beam is stable for separated turns. However, separated turns are not easily available in many heavy-ion cyclotrons because their acceleration voltages are insufficient compared with the large mass-to-charge ratio of the accelerated ions, or because of the high magnetic field employed in order to produce high-energy beams. The straightforward solution is to increase the acceleration voltage. At present, we operate the RF resonators of RRC at 18.25 MHz and the maximum available acceleration voltage is 0.28 MV/turn, which is insufficient to obtain separated turns. Hence usage of 24.33 MHz is proposed. In this case, an acceleration voltage increases up to 0.48 MV/turn, although we need some modifications for the present accelerator complex.

However, even in this case, effects from neighboring turns should be taken into account because they are not negligibly small. There are two methods to include the neighboring turn effects. The first is to impose a periodic boundary condition in the radial direction. This is justified for only a case of centering acceleration under a perfect isochronous magnetic field because coherent radial betatron motion or an imperfection of the isochronous magnetic field induces longitudinal misalignment of bunches. The other is to treat explicitly relevant neighboring bunches in the space-charge simulation. Yang et al. [59] pioneered space-charge simulation of this type using OPAL-CYCL, a "flavor" of the OPAL framework. Their result that neighboring turns reduce the transverse profile and the energy spread of the beam bunch is encouraging. So, we conducted multi-bunch simulations where a single Lorentz frame is used. It may be justified for $\gamma \approx 1$. Results for nearly centering acceleration are shown in Fig. 6. Compared with a result obtained by a single-bunch simulation under a periodic boundary condition, we find no drastic change in multi-bunch simulations. However, we found that simulation results fluctuate depending on the number of bunches included, that is, convergence is not yet obtained. It means that we need more bunches but it is difficult to increase the number of turns due to limitation of our computing resources at present. We need further studies on the effects of neighboring turns in order to understand quantitatively beam loss at extraction in heavy-ion cyclotrons.

SUMMARY

The "golden rule" for accelerating high-intensity beams in cyclotrons is to increase the acceleration voltage to obtain a sufficient turn separation at extraction so as to make maximal use of the local vortex motion. This was established by the success of PSI. To optimize the design of heavy-ion cyclotrons, a deeper understanding of neighboring-turn effects, both numerically and experimentally, is necessary.

REFERENCES

[1] R.S. Livingston, Proc. 5th Int. Cyclotron Conf., Oxford (1969) 423.
[2] A. Goto and Y. Yano (editors). Proceedings of the 17th Int. Conf. on Cyclotrons and their Applications, Tokyo (2004).
[3] G. Gulbekyan et al., Proc. 19th Int. Conf. Cyclotrons and their Applications, Lanzhou, China (2010) 33.
[4] for example, A. Denker et al., NIM B **240** (2005) 61.
[5] Y. Jongen et al., NIM A **624** (2010) 47.
[6] T. Abe et al., Plant Mutation Breeding and Biotechnology (Shu. Q.Y., ed.), The Joint FAO/IAEA programme (2010) pp. 95-102.
[7] Y. Yano, Proc. 12th Int. Conf. on Cyclotrons and their Applications, Berlin, Germany (1989) 13.
[8] L.M. Onishchenko, Phys. Part. Nuclei **39** (2008) 950.
[9] A. Goto, Proc. 19th Int. Conf. on Cyclotrons and their Applications, Lanzhou, China (2010) 9.
[10] E.O. Lawrence and N.E. Edlefsen, Science **72** (1930) 376.
[11] H.A. Bethe and M.E. Rose, Phys. Rev. **52** (1937) 1254.
[12] E.M. McMillan, Phys. Rev. **68** (1945) 143.
[13] V.I. Veksler, Phys. USSR **9** (1945) 153.
[14] J.R. Richardson et al., Phys. Rev. **69** (1946) 669.
[15] L.H. Thomas, Phys. Rev. **54** (1938) 580.
[16] M.K. Craddock, Proc. 19th Int. Conf. Cyclotrons and their Applications, Lanzhou, China (2010) 1.
[17] D.W. Kerst et al., Phys. Rev. **98** (1955) 1153.

ISBN 978-3-95450-173-1

[18] H.A. Willax, Proc. Int. Conf. on Sector-Focused Cyclotrons and Meson Factories, Geneva (1963) 386.
[19] V.P. Domitrievskii, "Relativistic Cyclotron with Space Variation of Magnetic Field", Report Presenting the Doctoral Dissertation Manuscript in Mathematical Physics, Dubna (1961).
[20] F.M. Russell, Nucl. Instr. and Meth. **23** (1963) 229.
[21] J. A. Martin, IEEE-NS-**13** (1966) 288.
[22] U. Trinks, Nucl. Instr. and Meth. **220** (1984) 186.
[23] L. Smith and A.A. Garren, "Orbit Dynamics in the Spiral-ridged Cyclotrons", UCRL-8598 (1959).
[24] K.R. Symon et al., Phys. Rev. **103** (1956) 1837.
[25] M. Seidel, "Cyclotrons for high-intensity beams", arXiv:1302.10011v1 [phyics.acc-ph] 5 Feb 2013.
[26] J. Grillenberger et al., Proc. 20th Int. Conf. Cyclotrons and their Applications, Vancouver, Canada (2013) 37.
[27] N. Fukunishi et al., Proc. 20th Int. Conf. on Cyclotrons and their Applications, Vancouver, Canada (2013) 1.
[28] F. Chautard et al., Proc. 19th Int. Conf. on Cyclotrons and their Applications, Lanzhou, China (2010) 16.
[29] J. Stetson et al., Proc. 19th Int. Conf. on Cyclotrons and their Applications, Lanzhou, China (2010) 27.
[30] H. Imao et al., Phys. Rev. ST Accel. Beams **15** (2012) 123501.
[31] H. Hasebe et al., INTDS-2014, Tokyo, Japan (2014).
[32] for example, A. Sen et al., Proc. 20th Int. Conf. on Cyclotrons and their Applications, Vancouver, Canada (2013) 420.
[33] G.G. Gulbekyan et al., Proc. 18th Int. Conf. on Cyclotrons and their Applications, (2007) 308.
[34] J.R. Richardson, Proc. 7th Int. Conf. Cyclotrons and their Applications, Basel, Switzerland (1975) 41.
[35] I. Strašík et al., Phys. Rev. ST Accel. Beams **13** (2010) 071004.
[36] W. Joho, Proc. 11th Int. Conf. Cyclotrons and their Applications, Tokyo, Japan (1986) 31.
[37] J.M. van Nieuwland, "Extraction of Particles from a Compact Isochronous Cyclotron", Doctoral thesis, Techinical Universiteit Eindhoven (1972).
[38] W. Joho, "Extraction of a 590 MeV Proton Beam from the SIN Ring Cyclotron", SIN-Report TM-11-8, Thesis (1970).
[39] V.P. Dmitrievsky et al., Proc. 9th Int. Conf. on Cyclotrons and their Applications, Caen, France (1981) 505.
[40] W. Joho, Part. Accel. **6** (1974) 41.
[41] M.M. Gordon, Proc. 5th Int. Cyclotron Conf., Oxford (1969) 305.
[42] Th. Stammbach, 13th Int. Conf. on Cyclotrons and their Applications, Vancouver, Canada (1992) 28.
[43] S. Adam, 14th Int. Conf. on Cyclotrons and their Applications, Cape Town, South Africa (1995) 446.
[44] R. Dölling, Proc. DIPAC2001, Grenoble (2001) 111.
[45] Th. Stammbach, 15th Int. Conf. on Cyclotrons and their Applications, Caen, France (1998) 369.
[46] W.J.G.M. Kleeven, "Theory of Accelerated Orbits and Space Charge Effects in an AVF Cyclotron", Doctoral thesis, Technische Universiteit Eindhoven (1988).
[47] F.J. Sacherer, Proc. PAC (1971) 1105.
[48] P. Bertrand and Ch. Ricaud, 16th Int. Conf. on Cyclotrons and their Applications, East Lansing, USA (2001) 379.
[49] I.M. Kapchinsky and V.V. Vladimirsky, Proc. Int, Conf. on High Energy Accelerators, CERN, Geneva (1959) 274.
[50] C. Chasman and A.J. Baltz, Nucl. Instrum. and Meth. Phys. Res. **219** (1984) 279.
[51] S.R. Koscielniak and S. Adam, Proc. 1993 Part. Accel. Conf., Washington, USA (1993).
[52] L.M. Onishchenko et al., NUKLEONIKA **48** (Supplement 2) (2003) S45-S48.
[53] E. Pozdeyev et al, Proc. Hadron Beam 2008, Nashville, Tennessee, USA (2008) 157.
[54] E.E. Perepelkin and S.B. Vorozhtsov, Proc. Of RuPAC 2997, Zvenigorod, Russia (2008) 40.
[55] A. Adelmann et al., Proc. ICAP09, San Francisco, CA, USA (2009) 107.
[56] R. Baartman, Proc. 20th Int. Conf. on Cyclotrons and their Applications, Vancouver, Canada (2013) 305.
[57] H. Okuno et al., IEEE Trans. Appl. Supercond., **17**, (2007) 1063.
[58] S.B. Vorojtsov et al., Proc. 16th Int. Conf. Cyclotrons and their Applications, East Lansing, USA (2001) 402.
[59] J.J. Yang et al., Phys. Rev. ST Accel. Beams **13** (2010) 064201.

ISBN 978-3-95450-173-1